A NIR Luminescent Copolymer Based on Platinum Porphyrin as High Permeable Dissolved Oxygen Sensor for Microbioreactors

Pengwei Jin, Ju Chu, Yu Miao, Jun Tan, Siliang Zhang, and Weihong Zhu
State Key Laboratory of Bioreactor Engineering, Key Laboratory for Advanced Materials and Institute of Fine Chemicals, East China University of Science and Technology, Shanghai 200237, P. R. China

DOI 10.1002/aic.14083
Published online March 22, 2013 in Wiley Online Library (wileyonlinelibrary.com)

Microbioreactors with multioptical sensors have become increasingly important because of their small working volumes, high degree of parallelization and the available robotics. A novel hydrophobic luminescent copolymer P(Pt-TPP-TFEMA) along with reference P(Pt-TPP-EMA) containing the pendant group of 5,10,15,20-tetraphenylporphyrin (TPP) moiety as low-cost dissolved oxygen (DO) chemosensor film for high-throughput microbioreactors is designed. Its sensor film exhibits fast response to DO with good stability and fatigue resistance, being capable of applying as a low-cost DO indicator for high-throughput bioprocess measurement. Results show that the quenching response of DO increases with the enhancement in the copolymeric hydrophobicity using the presented hybrid fluorinated ethyl methacrylate. Furthermore, the long emission band at 650 nm of chromophore TPP with large Stoke's shift about 250 nm brings several advantages, such as low scattering, deep penetration, and minimal interferences of absorption and fluorescence from the fermentation system, which shows high-promising application in bioprocess monitoring. © 2013 American Institute of Chemical Engineers *AIChE J*, 59: 2743–2752, 2013
Keywords: dissolved oxygen sensor, copolymer, platinum porphyrin, microbioreactor

Introduction

A fast, reliable and accurate monitoring of oxygen is extremely important for a wide range of applications such as environment, seawater, food industry, medicine and biotechnology.[1–7] The common determination of trace oxygen is based on amperometry (Clark electrode), which produces a small proportional current by consuming the oxygen content of the analyte in an electrochemical reaction.[8] Although Clark electrodes are sensitive and applicable to a wide temperature range, they are difficult to miniaturize with online monitoring.[9] The traditional fermentation bioreactors with large capacities are always equipped with dissolved oxygen (DO) electrodes, whereas they are quite incompetent to monitor high-throughput bioprocessing like small-scale fermentations for array microbioreactors. Moreover, the amperometry method presents multiple unresolved difficulties, such as the "static" reading, the expenses and changes in mixing dynamics when attaching DO electrodes to shake flasks. Given that the strain improvement as well as cell culture optimization is a labor-intensive process requiring a large number of parallel experiments under varying conditions, the conjunction of automated robotic systems with miniaturized DO detectors has become critical in the cell cultivation for low-cost high-throughput microbioreactors.[10–14] Consequently, the optical DO sensors based on the triplet-oxygen quenching of long-lived phosphorescence have become attractive with several advantages over traditional Clark electrodes, for instances, their small size and suitability for remote sensing and multiplex sensor networking.[15] Moreover, optical sensors do not consume oxygen, and are not easily poisoned like electrochemical detectors.[16] However, most reported cases for optical DO sensors are located in relatively short emission wavelength around 450–550 nm.[17,18] Obviously in monitoring high-throughput bioprocessing, the long wavelength emission of red or near-infrared (NIR) light is preferable, which exhibits specific advantages such as low scattering, low-energy radiation and minimal interferences of absorption and fluorescence from biological fermentation system.[19–21]

As a sensor film, the performances of optical sensors such as response time and stability are largely dependent on the supporting matrices and the oxygen-sensitive luminophores. Since most biological actions are carried out in aqueous system, optical DO film sensors with hydrophobicity are preferable in viewpoint of high-gas permeability and low pollution to reactors. The common methods are to physically or chemically dope the luminophores in polymers, sol–gel glass, and covalently bond to polymers.[22,23] Polystyrene (PS) and poly(methyl methacrylate) (PMMA) are widely used as the matrix, which plays a role in both hosting the oxygen-responsive luminophore and making oxygen penetrate from the surroundings. Introducing chemosensors into polymeric backbones via a covalent link can be easily fabricated into devices and chips fixed onto microbioreactors, along with

Correspondence concerning this article should be addressed to W. Zhu at whzhu@ecust.edu.cn.

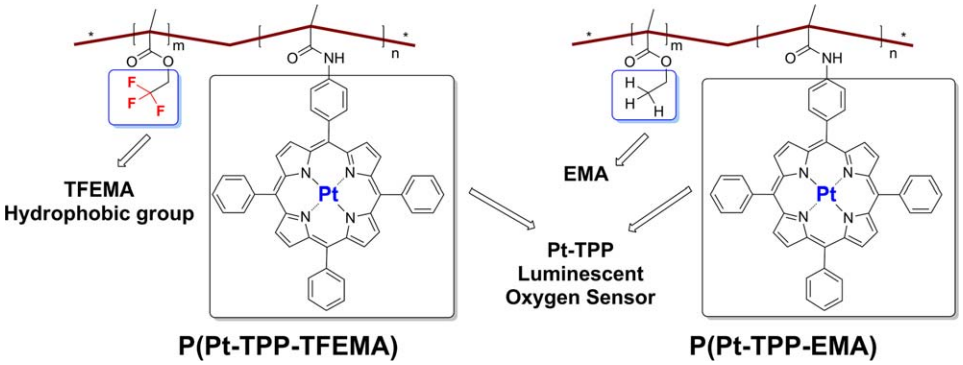

Scheme 1. Chemical structure of P (Pt-TPP-TFEMA) and reference P (Pt-TPP-EMA).

[Color figure can be viewed in the online issue, which is available at wileyonlinelibrary.com.]

avoiding the phase separation and concentration quenching of chromophores.[24] Recently, several copolymeric DO sensors have been exploited with using covalently immobilizable DO responsive chromophores.[25,26] On the basis of the high gas-permeability of fluorinated polymers,[27] we reported a NIR luminescent copolymer P(Pt-TPP-TFEMA) containing fluoro-substituted unit as DO sensor film, especially for high-throughput microbioreactors (Scheme 1). It was specifically synthesized from the copolymerization of a platinum complex of 5,10,15,20-tetraphenylporphyrin (TPP) with trifluoroethyl methacrylate (TFEMA). We found that the incorporated trifluoroethyl group into monomer TFEMA as the hydrophobic group can enhance the permeability of oxygen with high-responsive ability, which can be successfully applied as online DO measurements in fermentation system. The NIR luminescence with large Stoke's shift about 250 nm in sensing chromophore can effectively eliminate the interferences of absorption and fluorescence from biological fermentation system.

Experimental

Chemicals and instruments

^{1}H and ^{13}C NMR spectra were obtained by a Bruker AVANCE III 400 MHz Spectrometer. High-resolution mass spectra (HRMS) were determined by a Waters LCT Premier XE spectrometer. Absorption and fluorescence spectra were recorded on a Varian Cary 100 spectrometer and a HORIBA Scientific FluoroMax-4 spectrometer, respectively. The molecular weight and molecular weight distribution (M_w/M_n) were determined with a Waters 1515 Gel Permeation Chromatography (GPC) using THF as the mobile phase. Microsecond time resolved decay time data were acquired using an Edinburgh Instruments FLS900 fluorometer equipped with a microsecond flashlamp μF900. A 470 nm cutoff filter was used before the receiver to avoid the scattering of excitation light. The film was characterized by Atomic Force Microscope (AFM) with a MicroNano D 3000 scanning probe microscope.

Trifluoroethyl methacrylate was purchased from Aladdin Reagent Co., Ltd., and hydroquinone was used as the polymerization inhibitor before distillation. $PtCl_2$ was purchased from Jiuling Co., Ltd. (Shanghai). AIBN was recrystallized from anhydrous ethanol, and methacryloyl chloride was freshly prepared before use. All other chemicals used in this study were of analytical reagent grade. TPP, compounds 1, 2, 3 and methacryloyl chloride were prepared according to literature methods.[28–30]

Synthesis of P(TPP-TFEMA)

A mixture of compound 3 (80 mg, 0.11 mmol), TFEMA (1.9 g, 11.3 mmol), NMP (2.5 mL) and AIBN (4 mg, 0.024 mmol) was added to a Schlenk tube (25 mL) under an anhydrous oxygen-free condition at −78°C. The solution was degassed by three freeze–pump–thaw cycles, and stirred at 90–100°C for 18 h. The resulting mixture was transferred to a beaker, and purple sticky solid precipitated after petroleum ether (400 mL) was added. The solid was dissolved in CH_2Cl_2 (5 mL), precipitated in petroleum ether (400 mL), and the process was repeated for four times to obtain a light purple solid (1.45 g, yield 73.2%). P(TPP-EMA) was synthesized in the similar method.

Synthesis of P(Pt-TPP-TFEMA)

A mixture of benzonitrile (35 mL) and platinum dichloride (50 mg, 0.18 mmol) was refluxed for 4 h under argon protection. After cooling to room temperature, P(TPP-TFEMA) (1.0 g) was added, and continued to reflux for 3 h under argon atmosphere. The bulk solvent was evaporated, and the residual was poured into petroleum ether (100 mL). The solid was dissolved in CH_2Cl_2 (5 mL) and precipitated in petroleum ether (100 mL) twice. A red orange solid was obtained after vacuum drying (0.8 g, yield 76.2%). P(Pt-TPP-EMA) was synthesized in the similar method.

Microorganisms, medium and culture

Acremonium chrysogenum purchased from China General Microbiological Culture Collection Center with the accession number of CGMCC 3.4008, was grown on PMM agar medium (per liter: 10.0 g peptone, 12.0 g malt extract, 40.0 g maltose, 18.0 g agar; pH 7.0). The seed medium contained (per liter) 5.0 g glucose, 35.0 g sucrose, 50.0 g corn steep liquor, 0.5 g methionine, 8.0 g $(NH_4)_2SO_4$, 5.0 g $CaCO_3$ and 5.0 mL soybean oil; pH 6.5. The fermentation medium contained (per liter) 20.0 g glucose, 30.0 g starch, 50.0 g corn steep liquor, 6.0 g methionine, 13.0 g $(NH_4)_2SO_4$, 3.0 g urea, 3.0 g $MgSO_4{\cdot}7H_2O$, 9.0 g KH_2PO_4, 10.0 g $CaCO_3$, 40.0 mL soybean oil, 0.02 g $ZnSO_4{\cdot}7H_2O$, 0.02 g $CuSO_4{\cdot}5H_2O$, 0.02 g $MgSO_4{\cdot}7H_2O$ and 0.08 g $FeSO_4{\cdot}7H_2O$ under pH 6.2. *Acremonium chrysogenum* was precultured in several 500 mL shake flasks containing 50 mL seed medium at 28°C and 220 rpm for 3 days. 10% (v/v) precultures were inoculated in microbioreactor at 28°C.

Preparation of DO sensor film

The DO sensor films based on luminescent P(Pt-TPP-TFEMA) and reference P(Pt-TPP-EMA) were prepared by

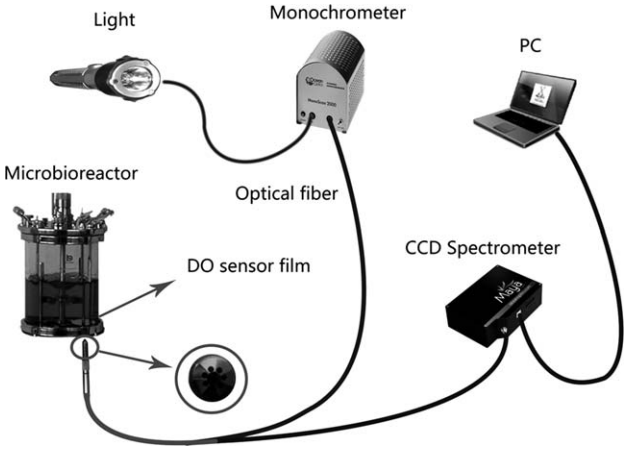

Figure 1. Schematic diagram of DO sensing system for luminescence spectra.

spin-coating a 5 wt % toluene solution on a thoroughly-washed quartz substrate. The film border was fixed by strips of adhesive tape. An AFM was employed to visualize the surface, and to measure the thickness of the film roughly. The sensor film was estimated at about 500 nm.

Spectral determination of copolymeric film on DO response

The film-coated quartz as a sensor patches was firmly attached onto the bottom of the custom-made microbioreactor. A QF600-8-VIS/NIR bifurcated optic fluorescence fiber bundle from Ocean Optics was used to realize the portable online and noninvasive monitoring (Figure 1). The optic probe contains one flat fiber for detection, and seven angled fibers that direct excitation energy to the region in front of the detection fiber. Therefore, the optic probe combines excitation and detection in one optical fiber for avoiding the interfering effect of total-reflected light in the traditional 90-degree optical design for the light source and detector. Moreover, the large Stoke's shift about 250 nm can effectively eliminate the interference of the excitation light during the detection of luminescence emission. The signal acquiring time was set as 0.1 s with fixed integration numbers.

To prepare a range of DO concentrations for work plot, the deionized water was saturated with various mixture gases under constant stirring. A gas blender was used to prepare the oxygen mixtures. The DO concentration was monitored by a YSI model 5000 dissolved oxygen meter.

DO sensing principles

The DO luminescent sensing can be described by classical Stern-Volmer equation (Eq. 1)

$$\frac{I_0}{I}=\frac{\tau_0}{\tau}=1+K_{\mathrm{D}}[Q] \tag{1}$$

where I_0 and τ_0 are the initial luminescent intensity and lifetime of phosphorescent dyes in an inert atmosphere, I and τ are the luminescent intensity and lifetime in the presence of O_2, respectively. K_{D} is the Stern–Volmer quenching constant, and $[Q]$ is the concentration of O_2.

For heterogeneous luminescent O_2 sensing, the quenching curves are analyzed by data fitting into two components, namely, the homogeneously distributed and the heterogeneously distributed forms.[31] The two-site model Stern–Volmer equation with two discrete sets of quenching parameters is described as follows (Eq. 2)

$$\frac{I}{I_0}=\frac{\tau}{\tau_0}=\frac{f_1}{1+K_{\mathrm{sv}}^1[O_2]}+\frac{f_2}{1+K_{\mathrm{sv}}^2[O_2]} \tag{2}$$

where f_1 and f_2 are the fractions of the total emission for each component, respectively (with f_1+f_2 being 1). K_{sv}^1 and K_{sv}^2 are the Stern–Volmer constants for each component.

Results and Discussion

Design and synthesis of P(Pt-TPP-TFEMA)

The sensitivity of an optical oxygen sensor is mainly dependent on the ability of oxygen to quench the probe luminescence with three characteristics (1) the long lifetime with excited states in the absence of oxygen favors the creation of sensitive oxygen sensors, (2) the higher film permeability toward oxygen results in more sensitivity to oxygen, and (3) the higher quenching efficiency to oxygen leads to higher sensitivity. Ideally, the best situation is that the excited states of luminescent probe molecules are quenched once it encounters an oxygen molecule.[32] Based on these aspects, we choose Pt complexes of porphyrin derivatives as candidates in that they show long wavelength phosphorescence at room temperature, visible light excitation and large Stoke's shift.[33] Moreover, their long excited-state lifetime up to microseconds is another key point for good candidates as optical oxygen probes.[34]

The DO sensors studied to date have predominantly focused on physically doping the luminophores within the polymer or sol–gel matrix as the supporter, which can lead to the serious phase-separation and leaching problems. Accordingly, there is a practical advantage to incorporate luminophore via covalently bonding to the matrix.[35] In addition; the fluorescence self-quenching induced by aggregation can be efficiently avoided by adjusting the molar ratio between the monomers of luminophore and matrix.

In general, the film containing fluorocarbon group has a high permeability to oxygen. Also, fluorinated copolymers have some unique properties such as good biocompatibility, high thermal stability, photo-oxidation stability, good chemical resistance, superior hydrophobility and low refractive index.[25] With these considerations, we selected TFEMA containing trifluoroethyl group as matrix monomer for the sake of enhancing the permeability of oxygen, specifically copolymerized with a long wavelength luminophore of Pt porphyrin complex (Scheme 2). Meantime, an ethyl methacrylate (EMA) was used as a reference. For the synthetic strategy, the sensing luminophore is functionalized with a pendent vinyl group to provide an accessible site for polymerization. Generally, polymers could be obtained by solution, suspension and UV-free-radical polymerization. In this work, solution polymerization was conducted in preparing the target copolymer P(Pt-TPP-TFEMA) and P(Pt-TPP-EMA) due to its easiness in operation.

The intensive ligand absorption around 410 nm (Figure 2a) is from the Soret band (B band, $S_0 \rightarrow S_3$ transition), and the weak absorption from 500 to 600 nm is the Q band ($S_0 \rightarrow S_1$ and $S_0 \rightarrow S_2$ transitions). The disappeared minor absorption bands of the free ligand at 550 to 650 nm are indicative of the successful coordination between Pt with TPP.[36] The disappearance of ^{1}H NMR peak around -2.8 ppm in upfield further proves the successful coordination

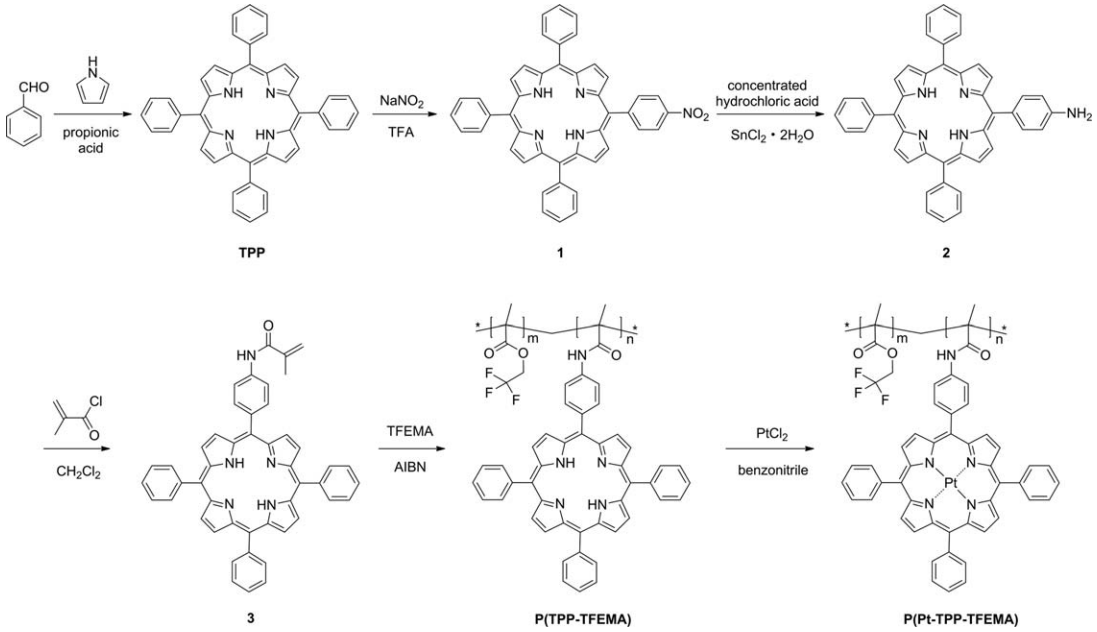

Scheme 2. Synthesis of copolymer P(Pt-TPP-TFEMA).

(Figure 2b). The weight-average molecular weight (M_w) for P(Pt-TPP-TFEMA) and P(Pt-TPP-EMA) determined by GPC is 107,265 and 94,154, with a polydispersity of 1.1 and 1.2, respectively. The molar ratio of two monomers could be determined from the standard working curve or calibration curve in the absorption spectra, which confirmed the molar ratio of monomer 3 to monomer TFEMA as 1:157 in copolymer P(TPP-TFEMA), and to monomer EMA for 1:128 in copolymer P(TPP-EMA), respectively. As discussed later, the molar ratio (ca. 1:150) between luminophore vs. matrix monomer can exhibit ideal luminescence, which can be successfully exploited to online monitor DO in the fermentation system.

Optical response of sensing films to DO

The luminescent properties of copolymers P(Pt-TPP-EMA) and P(Pt-TPP-TFEMA) were studied in saturated N_2, air and O_2 states, respectively. In order to make a convincing comparison of these two polymers, the concentrations of the porphyrin units were carefully controlled on the same level in each polymer solution. The polymeric quenching response to DO is defined as Q_{DO} (Eq. 3)

$$Q_{DO} = I_0 / I_{100} \tag{3}$$

where I_0 and I_{100} are corresponding to the luminescent signals in saturated N_2 and O_2 system, respectively. For P(Pt-TPP-TFEMA), it was found that the emission intensity was quenched by about 8-fold in saturated O_2 acetonitrile solution with respect to that in saturated N_2 solution ($Q_{DO} = 8$, Figure 3b). For the P(Pt-TPP-EMA), however, the emission intensity was reduced by about 6-fold in saturated O_2 acetonitrile solution ($Q_{DO} = 6$, Figure 3a). Similarly, the O_2 sensitivities for the polymer film state were investigated. Although the O_2 quenching effect in the copolymeric film sate is not as remarkable as in acetonitrile solution due to the difference in O_2 diffuse speed, it is still enough to

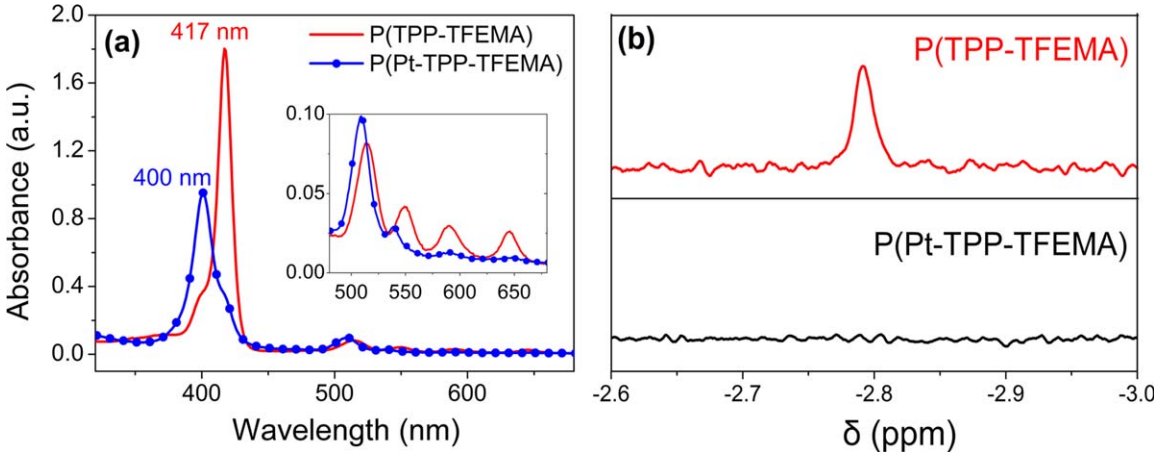

Figure 2. (a) Absorption spectra of P(TPP-TFEMA) and P(Pt-TPP-TFEMA) in CH_2Cl_2. Inset: Partial enlarged drawing of minor peaks, and (b) partial enlarged ^1H NMR spectra of P(TPP-TFEMA) and P(Pt-TPP-TFEMA) in $CDCl_3$.

[Color figure can be viewed in the online issue, which is available at wileyonlinelibrary.com.]

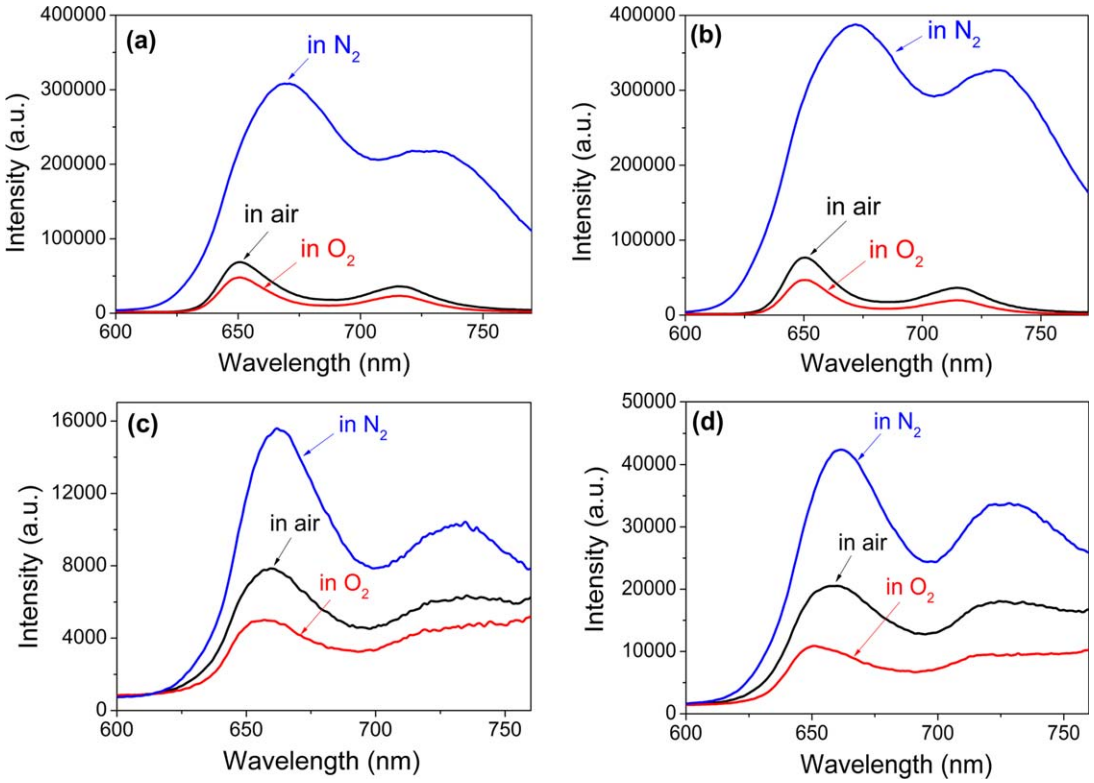

Figure 3. Luminescence intensity of Pt complex polymers in saturated N_2, air and O_2 acetonitrile solution and films (water for film medium) on excitation at 405 nm.

(a) P(Pt-TPP-EMA), $Q_{DO} = 6$, (b) P(Pt-TPP-TFEMA), $Q_{DO} = 8$, (c) P(Pt-TPP-EMA) film, $Q_{DO} = 3$, and (d) P (Pt-TPP-TFEMA) film, $Q_{DO} = 4$. [Color figure can be viewed in the online issue, which is available at wileyonlinelibrary.com.]

exhibit the specific response to the concentration of DO. For P(Pt-TPP-EMA) and P(Pt-TPP-TFEMA), the polymeric quenching responses to DO (Q_{DO}) were 3 and 4 (Figure 3c and d), respectively. Obviously, the incorporation of trifluoroethyl group into the matrix can increase the quenching effects (Q_{DO}) both in solution and film states, which is indicative that P(Pt-TPP-TFEMA) is more sensitive to the presence of O_2 than that of P(Pt-TPP-EMA).

The DO response time of the copolymer films was further studied in water (Figure 4, the response time was measured when 95% emission intensity was changed). The water system was saturated with N_2 and O_2 in turn for 5 cycles, and the phosphorescence was monitored per second. Comparing with P(Pt-TPP-EMA), P(Pt-TPP-TFEMA) can be toggled repeatedly between the saturated N_2 and O_2, and remained intact without obvious change (Figures 4a and 4b). Obviously, the reproducibility and recycling ability of P(Pt-TPP-TFEMA) is better than that of P(Pt-TPP-EMA). The response time of P(Pt-TPP-EMA) to O_2 and N_2 were 4 min and 6 min (Figure 4c), respectively. In contrast, the response time of P(Pt-TPP-TFEMA) (Figure 4d) were about 5 times faster in detecting DO from saturated N_2 state (50 s), and 3 times faster from saturated O_2 state (2 min), respectively. Generally, incorporation of fluoro-substituted group into polymeric matrix always increases the hydrophobicity of fluorinated polymers.[8] C—F bonds can reduce overall molecular polarizabilities of organic molecules by increasing the hardness of the carbon framework, a fact that helps account for the general increase in lipophilicity.[37] Therefore, we consider that the increased oxygen permeability in aqueous system is predominately attributed to the hydrophobicity from fluoro-substituted group. Moreover, compared with P(Pt-TPP-EMA), the value of Q_{DO} and luminescence of P(Pt-TPP-TFEMA) kept stable after the film was irradiated by the light of 405 nm for 2 h (Figure 5a, the film was irradiated every 10 s in saturated N_2 water, and in the rest of time the shuttle before the light was closed), and no significant change or degradation was observed over a one-month period under ambient air. It is indicative of satisfying the long-time process in microbioreactors.

For gas-phase oxygen detection, the sensor sensitivity is dependent on the oxygen diffusion coefficient within the film, and the oxygen solubility coefficient within the film is a minor factor. However, for DO detection, the sensitivity is dependent on both the oxygen diffusion coefficient and the oxygen solubility coefficient within the film. It has been demonstrated that the film hydrophobicity plays an essential role in sensor operation in aqueous system.[38] Due to the relatively low solubility (ca. 9.2 ppm with air equilibrium) of oxygen in water, a hydrophobic film could enhance the DO quenching process by reducing water solubility in the matrix and causing the partitioning of oxygen out of solution into the gas phase within the sensing film. As a result, the hydrophobic film based on P(Pt-TPP-TFEMA) can enhance oxygen diffusion on the polymer sensing system, improve the sensor sensitivity, and fatigue resistance.

To establish the relationship between oxygen concentration and film luminescence, the work plot was conducted afterwards (Figure 5b). Here the oxygen sensing data of P(Pt-TPP-EMA) and P(Pt-TPP-TFEMA) were fitted with the two-site model, and the corresponding fitting data were summarized in Table 1. The experimental results in Figure 5b

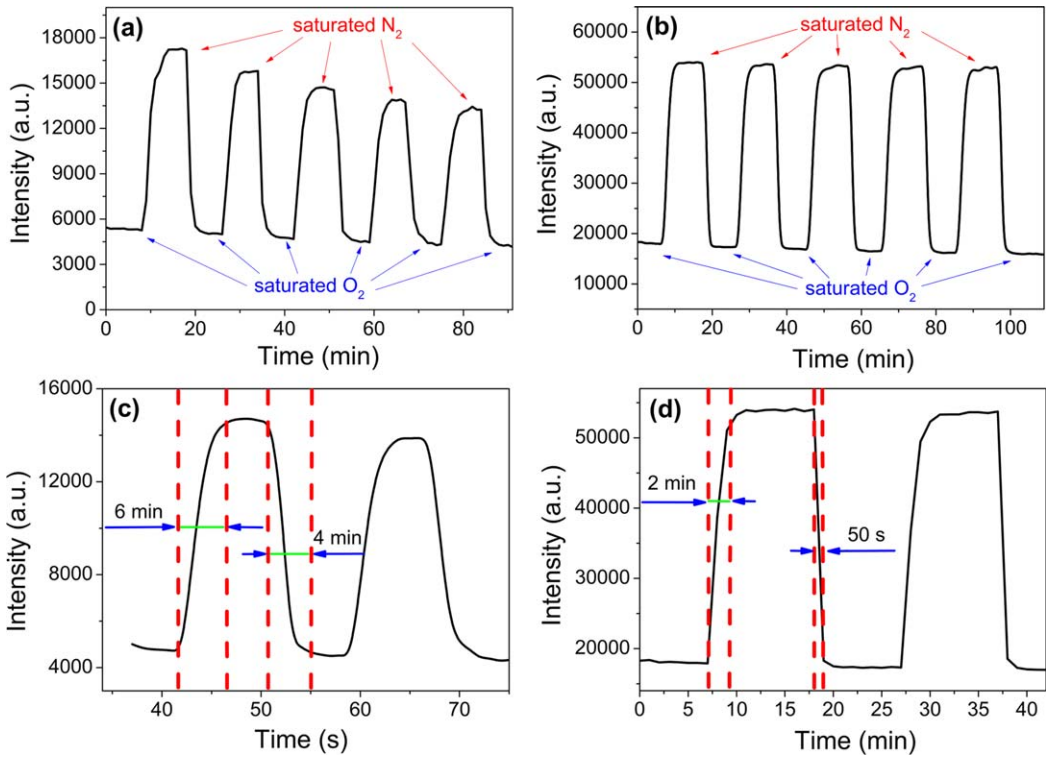

Figure 4. Luminescence intensity response of Pt complex polymers in water to O_2/N_2 switching cycles upon excitation at 405 nm and emission at 650 nm.

(a) P(Pt-TPP-EMA), (b) P(Pt-TPP-TFEMA), (c) and (d) are partial enlarged drawing of (a) and (b), respectively. [Color figure can be viewed in the online issue, which is available at wileyonlinelibrary.com.]

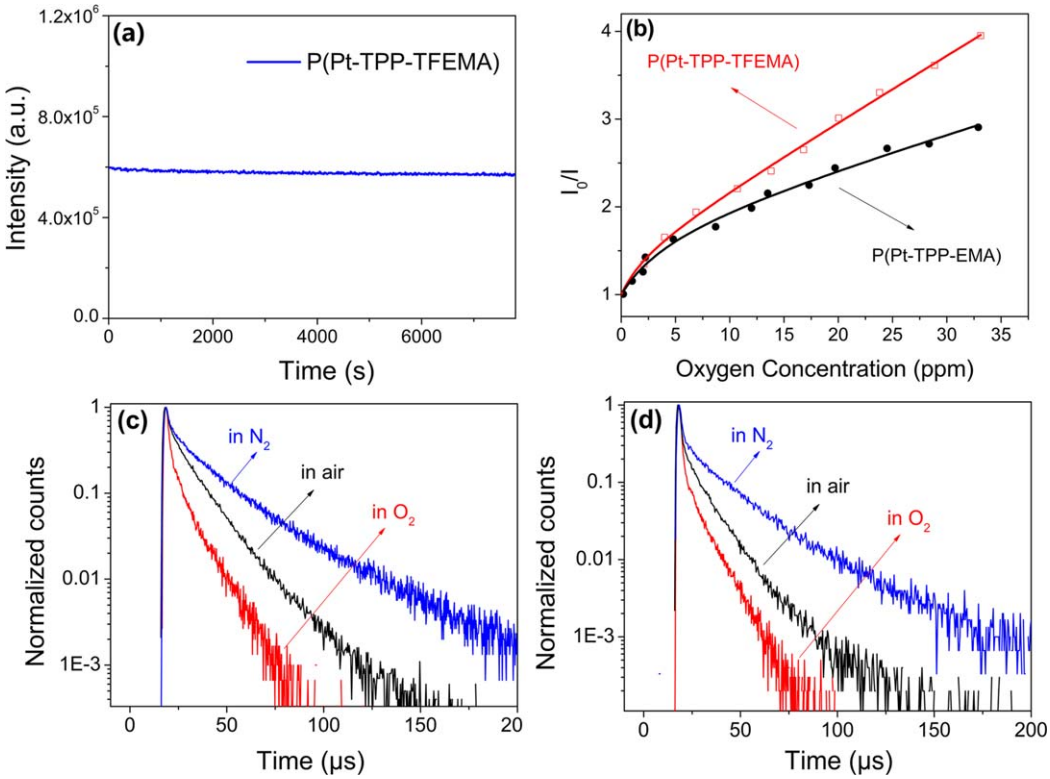

Figure 5. (a) Photostability test of P(Pt-TPP-TFEMA) film; (b) Two-site model fit plots of P(Pt-TPP-TFEMA) and P(Pt-TPP-EMA).

Luminescence lifetime of Pt complex film in saturated N_2, air and O_2 water upon excitation at 405 nm and emission at 650 nm, (c) P(Pt-TPP-EMA), and (d) P(Pt-TPP-TFEMA). [Color figure can be viewed in the online issue, which is available at wileyonlinelibrary.com.]

Table 1. Parameters of the Fitting Result in the Emission Intensity with the Two-Site Model for P(Pt-TPP-EMA) and P(Pt-TPP-TFEMA) Film.

film	[a]f_1	[a]f_2	[b]K_{sv}^1	[b]K_{sv}^2	[c]r^2
P(Pt-TPP-EMA)	0.51	0.49	0.384	0.019	0.991
P(Pt-TPP-TFEMA)	0.40	0.60	0.603	0.047	0.997

[a]The ratio of the two portions in the two-site model.
[b]The quenching constants of the two portions (ppm^{-1}).
[c]The determination coefficients.

reveal that the curve in the low-oxygen concentration shows nonlinearity while it shows linearity in the high-oxygen concentration higher than 10 ppm. Obviously, the high slope of line is an indication of high DO sensitivity. In contrast to homogeneous solutions, usually the microenvironment of the polymer matrix is not the same for all dye molecules on an averaged time scale, leading to a multiexponential or even nonexponential excited state decay.[39] At the low-oxygen concentration, only the most accessible luminophore molecules can interact with oxygen, and lead to high sensitivity; whereas at the high-oxygen concentration, the easily accessible luminophore molecules are largely quenched, and the quenching sensitivity is dominated by the luminophore molecules in the less accessible areas.[40]

Luminescence lifetimes of DO sensing films

Given that the unique properties of Pt porphyrin complexes, the luminescence lifetimes of DO sensing films were investigated in saturated N_2, air and O_2 state, respectively. It was found that the luminescence lifetime curves were best fitted by a double exponential decay equation (Eq. 4, Figure 5c and d)

$$R(t)=A_1 e^{-\frac{t}{\tau_1}}+A_2 e^{-\frac{t}{\tau_2}} \tag{4}$$

The molar contribution of the lifetime can commonly be calculated by Eq. 5, where A_i stands for the amplitude of exponential decay equation and τ_i stands for the lifetime. Since the copolymeric system obeys double exponential decay, Eq. 5 can be simplified to Eq. 6

$$\alpha_i=\frac{A_i\tau_i}{\sum_{i=1}^{n}A_i\tau_i} \tag{5}$$

$$\alpha_{1(2)}=\frac{A_{1(2)}\tau_{1(2)}}{A_1\tau_1+A_2\tau_2} \tag{6}$$

Given that α_1 and α_2 are far more than 3% (Table 2), it cannot be ignored as an error from a single exponential decay. In addition, the double exponential decay shows that there are two processes in the luminescence decay. The two processes can be designated as oxygen-easy accessible site and oxygen-difficult accessible site quenching, respectively. As expected, the plot of luminescence intensity shows a higher ratio (I_0/I_{100}) than the decay time plot (τ_0/τ_{100}), which is quite common for the optical oxygen sensors.[1]

In general, there are two common modes for monitoring DO: fluorescence intensity method and fluorescence lifetime measurement. The former mode is widely used because of its simple and inexpensive feature. Although the measurement in fluorescence intensity has some disadvantages such as the drift of light source and detector, and the change due to degradation or leaching of the sensor dye, these shortcomings could be effectively avoided by calibration, photostable sensors and optimizing matrix. Fluorescence lifetime is an important parameter of fluorophore which is independent of molecular concentration. However, the fluorescence lifetime measurement requires sophisticated instruments with little suitability for practical application in high-throughput bioprocessing at this stage.[41]

Potential application

Finally, the DO sensing film of P(Pt-TPP-TFEMA) was applied in *cephalosporin C* fermentation system to check the possibility of continuous online measurements of DO. Since there's no DO electrode available in microbioreactors, the fermentation broth has to be taken out for rough measurement. However, many fermentation broths such as *cephalosporins acremonium* consume oxygen very fast, and the oxygen level will drop to near zero once the flask stop shaking or microbioreactor stop bubbling. Therefore, it is unable to measure the DO in real-time unless constructing an online setup. Accordingly, we checked the possibility of detecting DO in fermentation broth using our online setup. *Cephalosporin C* fermentation broth was transferred from other fermentation tank to our microbioreactor and saturated with N_2 for 10 min. Then O_2 was bubbled into the microbioreactor at a certain speed until the fermentation was saturated by O_2, and fluorescence was monitored at short intervals (1 s, Figure 6a). As expected, the luminescence became weak upon increasing the O_2 contents. Traditional right-angle method of fluorometer cannot fulfill the task since a certain angle of the sensing film is installed to receive the excitation light and reflect the emission light. Because *cephalosporin C* fermentation broth is very viscous fluid, it is not so easy for a light to penetrate through, and the fermentation will scatter both excitation and emission light seriously. Fortunately, our setup can avoid these problems, in which the sensing film patch was attached onto the bottom of the microbioreactor with film side facing to the inside. The optical fiber can easily detect the luminescence without interference. As shown in Figure 6a, the tendency in fluorescent change indicates that the DO sensor film based on P(Pt-TPP-TFEMA) has a broad response in application for microbioreactors.

Furthermore, in order to assess the utility of the proposed method, it was successfully applied to the online determination of DO during fermentation in microbioreactor. The film patch was attached onto the microbioreactor, and the fermentation was cultivated as usual. The luminescence was monitored, and a parallel experiment was conducted in a

Table 2. Parameters of Luminescence Lifetime of DO Sensing for P(Pt-TPP-EMA) and P(Pt-TPP-TFEMA) Films.

film	[a]condition	τ_1 (μs)	τ_2 (μs)	[b]α_1 (%)	[b]α_2 (%)
P(Pt-TPP-EMA)	O_2	1.5	8.3	14.9	85.1
	air	2.0	13.2	13.6	86.4
	N_2	1.6	19.2	5.8	94.2
P(Pt-TPP-TFEMA)	O_2	0.8	6.8	19.6	80.4
	air	2.5	11.1	11.8	88.2
	N_2	1.5	20.8	17.2	82.8

[a]The water was saturated with specific gas over 30 min.
[b]α_1 and α_2 are the fractions of the total emission for each component, respectively (with $\alpha_1 + \alpha_2$ being 1).

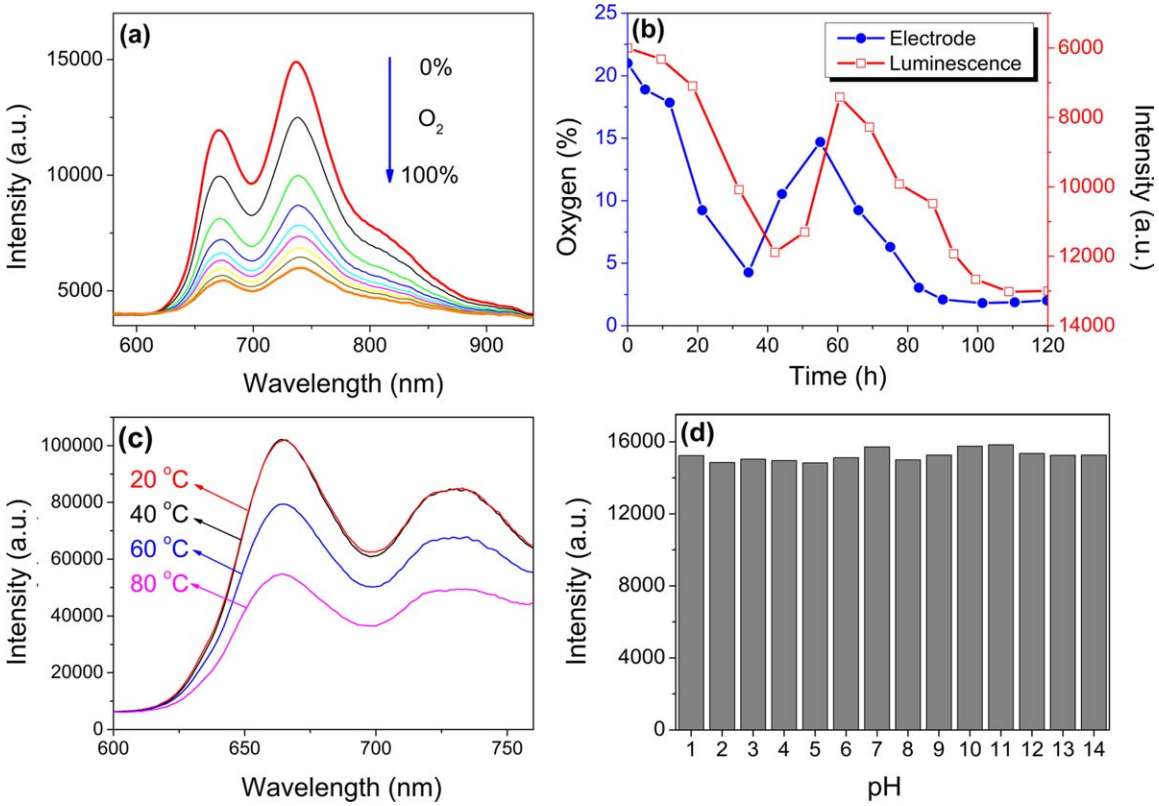

Figure 6. (a) Phosphorescent emission intensity of P(Pt-TPP-TFEMA) film in *cephalosporin C* fermentation with increasing O_2 contents after saturated with nitrogen.

$\lambda_{ex} = 405$ nm, $Q_{DO} = 2.5$; (b) Online monitoring of DO in *cephalosporin C* fermentation broth monitored by electrode equipped in traditional fermentation bioreactor and DO sensing film. Luminescence intensity response of P(Pt-TPP-TFEMA) film upon excitation at 405 nm in saturated N_2 water along with (c) temperature (20–80°C), and (d) pH (monitored at 670 nm). [Color figure can be viewed in the online issue, which is available at wileyonlinelibrary.com.]

traditional fermentation bioreactor equipped with DO electrode (Figure 6b). Both of the fermentation remained in the same condition as far as possible except for reactor volume. The variation trends of the two measurements were in good agreement (Figure 6b, the luminescent intensity is reversed vertically for convenience of comparison), which further confirmed the potential application in microbioreactors. The DO profile of the fermentation first declined to its valley value due to the cell growth making use of starch as the carbon source, and then had a DO rise because of the exhaustion of starch before the oil was induced to be used as the second carbon source. When the oil was started to be used, the DO dropped again starting from the peak value, since *Acremonium chrysogenum* consumed large amounts of oxygen in making use of soybean oil. Utilizing the job's plot, the luminescence can be converted to DO content quantitatively.

In order to enable the sensor films to qualify as microbioreactor oxygen sensors, we should demonstrate that this copolymeric sensor only picks up DO rather than other species (pH or temperature). The temperature effect on the luminescence of P(Pt-TPP-TFEMA) film was further studied, which indicated that the luminescence intensity became decreased with an increase in temperature (Figure 6c). However, during the on-line measurement in *cephalosporin C* fermentation system, the fermentation temperature is always kept between 25–28°C. Accordingly, the effect of temperature change can be neglected since the little luminescence changes from 20 to 40°C. Of course, a correction factor might be needed when it is exploited in a wide temperature variation window. Moreover, the pH has no effect on the luminescence of film (Figure 6d). Meantime, in *cephalosporin C* system, the pH rises from 6.5 to 7.0 at the onset of fermentation, and then stabilizes at 5.5, with minute interference on the copolymeric luminescence. Obviously, the effect of pH and temperature can be ruled out during the continuous online measurements of DO in *cephalosporin C* fermentation system. Accordingly, with the easiness in synthesis, low price, long wavelength and fast response to DO, the chemosensor film of P(Pt-TPP-TFEMA) could be potentially applied as a low-cost microbioreactor DO indicator for high-throughput bioprocessing. Here the long wavelength emission approaching NIR range could ensure low scattering and minimal interfering from biological fermentation samples.[42–45]

Conclusions

In summary, a long wavelength luminescent hydrophobic copolymer P(Pt-TPP-TFEMA) was developed as DO chemosensor for bioprocess monitoring, in which a covalently immobilizable Pt-TPP chromophore is used as DO-sensitive unit. In the target polymeric chemosensor system, the monomer of TFEMA containing trifluoroethyl unit is chosen as the main polymeric matrix due to its high hydrophobicity. The copolymeric sensor film shows high sensitivity to DO

with good fatigue resistance. The long wavelength emission approaching NIR range could ensure low scattering and minimal interfering from biological fermentation samples. Due to the good oxygen permeation, the chemosensor film of P(Pt-TPP-TFEMA) is successfully applied as a low-cost microbioreactor DO indicator for high-throughput bioprocessing.

Acknowledgments

The authors thank NSFC/China, National 973 Program (2013CB733700), the Oriental Scholarship, the Fundamental Research Funds for the Central Universities (WK1013002), National Major Scientific Technological Special Project (2012YQ15008709), the doctoral program of higher education of specialized research fund (20110074110015), and the Open Funding Project of the State Key Laboratory of Bioreactor Engineering for providing financial support to this project.

Literature Cited

1. Borisov SM, Klimant I. Ultrabright oxygen optodes based on cyclometalated iridium(III) coumarin complexes. *Anal Chem*. 2007;79:7501–7509.
2. Benziger J, Kimball E, Mejia-Ariza R, Kevrekidis I. Oxygen mass transport limitations at the cathode of polymer electrolyte membrane fuel cells. *AIChE J*. 2011;57:2505–2517.
3. Zhukovsky KV. Three dimensional model of oxygen transport in a porous diffuser of a PEM fuel cell. *AIChE J*. 2003;49:3029–3036.
4. Zhukovsky KV, Zhukovsky VC. 3-Dimensional model of oxygen-nitrogen transport in porous diffuser of polymer electrolyte hydrogen fuel cell. *Moscow University Physics Bulletin C/C of Vestnik-Moskovskii Universitet Fizika I Astronomiia;* 2002;57:32–40.
5. Zhukovsky K. Modeling of the current limitations of PEFC. *AIChE J*. 2006;52:2356–2366.
6. Zhukovsky K, Pozio A. Maximum current limitations of the PEM fuel cell with serpentine gas supply channels. *J Power Sources*. 2004;130:95–105.
7. Zou X, Hang HF, Chu J, Zhuang YP, Zhang SL. Oxygen uptake rate optimization with nitrogen regulation for erythromycin production and scale-up from 50 L to 372 m^3 scale. *Bioresource Technol*. 2009;100:1406–1412.
8. Xiong Y, Xu J, Zhu DQ, Duan CF, Guan YF. Fiber-optic fluorescence sensor for dissolved oxygen detection based on fluorinated xerogel immobilized with ruthenium (II) complex. *J Sol-Gel Sci Technol*. 2010;53:441–447.
9. Ramamoorthy R, Dutta PK, Akbar SA. Oxygen sensors: materials, methods, designs and applications. *J Mater Sci*. 2003;38:4271–4282.
10. Schäpper D, Alam M, Szita N, Lantz AE, Gernaey K. Application of microbioreactors in fermentation process development: a review. *Anal Bioanal Chem*. 2009;395:679–695.
11. Amanullah A, Otero JM, Mikola M, Hsu A, Zhang JY, Aunins J, Schreyer HB, Hope JA, Russo AP. Novel micro-bioreactor high throughput technology for cell culture process development: reproducibility and scalability assessment of fed-batch CHO cultures. *Biotechnol Bioeng*. 2010;106:57–67.
12. Hortsch R, Stratmann A, Weuster-Botz D. New milliliter-scale stirred tank bioreactors for the cultivation of mycelium forming microorganisms. *Biotechnol Bioeng*. 2010;106:443–451.
13. Wu D, Hao YY, Chu J, Zhuang YP, Zhang SL. Inhibition of degradation and aggregation of recombinant human consensus interferon-α mutant expressed in Pichia pastoris with complex medium in bioreactor. *Appl Microbiol Biotechnol*. 2008;80:1063–1071.
14. Wang ZJ, Wang HY, Li YL, Chu J, Huang MZ, Zhuang YP, Zhang SL. Improved vitamin B12 production by step-wise reduction of oxygen uptake rate under dissolved oxygen limiting level during fermentation process. *Bioresource Technol*. 2010;101:2845–2852.
15. Chen RS, Farmery AD, Obeid A, Hahn CEW. A cylindrical-core fiber-optic oxygen sensor based on fluorescence quenching of a platinum complex immobilized in a polymer matrix. *IEEE Sens J*. 2012;12:71–75.
16. Wu CF, Bull B, Christensen K, McNeill J. Ratiometric single-nanoparticle oxygen sensors for biological imaging. *Angew Chem Int Ed*. 2009;48:2741–2745.
17. Huynh L, Wang Z, Yang J, Stoeva V, Lough A, Manners I, Winnik MA. Evaluation of phosphorescent rhenium and iridium complexes in polythionylphosphazene films for oxygen sensor applications. *Chem Mater*. 2005;17:4765–4773.
18. DeRosa MC, Hodgson DJ, Enright GD, Dawson B, Evans CEB, Crutchley RJ. Iridium luminophore complexes for unimolecular oxygen sensors. *J Am Chem Soc*. 2004;126:7619–7626.
19. Huang XH, El-Sayed IH, Qian W, El-Sayed MA. Cancer cell imaging and photothermal therapy in the near-infrared region by using gold nanorods. *J Am Chem Soc*. 2006;128:2115–2120.
20. Guo ZQ, Zhu WH, Tian H. Dicyanomethylene-4*H*-pyran chromophores for OLED emitters, logic gates and optical chemosensors. *Chem Commun*. 2012;48:6073–6084.
21. Zhu WH, Huang XM, Guo ZQ, Wu XM, Yu HH, Tian H. A novel NIR fluorescent turn-on sensor for the detection of pyrophosphate anion in complete water system. *Chem Commun*. 2012;48:1784–1786.
22. Zhao Q, Li FY, Huang CH. Phosphorescent chemosensors based on heavy-metal complexes. *Chem Soc Rev*. 2010;39:3007–3030.
23. Kim HN, Guo ZQ, Zhu WH, Yoon J, Tian H. Recent progress on polymer-based fluorescent and colorimetric chemosensors. *Chem Soc Rev*. 2011;40:79–93.
24. Shen LJ, Lu XY, Tian H, Zhu WH. A long wavelength fluorescent hydrophilic copolymer based on naphthalenediimide as pH sensor with broad linear response range. *Macromolecules*. 2011;44:5612–5618.
25. Tian YQ, Shumway BR, Meldrum DR. A new crosslinkable oxygen sensor covalently bonded into poly(2-hydroxyethyl methacrylate)-*co*-polyacrylamide thin film for dissolved oxygen sensing. *Chem Mater*. 2010;22:2069–2078.
26. Borisov SM, Lehner P, Klimant I. Novel optical trace oxygen sensors based on platinum (II) and palladium (II) complexes with 5,10,15,20-*meso*-tetrakis-(2,3,4,5,6-pentafluorphenyl)porphyrin covalently immobilized on silica-gel particles. *Anal Chim Acta*. 2011;690:108–115.
27. He GP, Zhang GW, Hu JW, Sun JP, Hu SY, Li YH, Liu F, Xiao DS, Zou HL, Liu GJ. Low-fluorinated homopolymer from heterogeneous ATRP of 2,2,2-trifluoroethyl methacrylate mediated by copper complex with nitrogen-based ligand. *J Fluorine Chem*. 2011;132:562–572.
28. Mathew S, Johnston MR. The synthesis and characterisation of a free-base porphyrin-perylene dyad that exhibits electronic coupling in both the ground and excited states. *Chem Euro J*. 2009;15:248–253.
29. Luguya R, Jaquinod L, Fronczek FR, Vicente MGH, Smith KM. Synthesis and reactions of *meso*-(p-nitrophenyl)porphyrins. *Tetrahedron*. 2004;60:2757–2763.
30. Lembo A, Tagliatesta P, Cicero D, Leoni A, Salvatori A. A glycyl-substituted porphyrin as a starting compound for the synthesis of a π–π-stacked porphyrin-fullerene dyad with a frozen geometry. *Org Biomol Chem*. 2009;7:1093–1096.
31. Klimant I, Wolfbeis OS. Oxygen-sensitive luminescent materials based on silicone-soluble ruthenium diimine complexes. *Anal Chem*. 1995;67:3160–3166.
32. Mills A. Optical oxygen sensors utilising the luminescence of platinum metals complexes. *Platinum Met Rev*. 1997;41:115–127.
33. Chu CS, Lo YL. High-performance fiber-optic oxygen sensors based on fluorinated xerogels doped with Pt(II) complexes. *Sensor Actuators B*. 2007;124:376–382.
34. Che CM, Hou YJ, Chan MCW, Guo JH, Liu Y, Wang Y. [*meso*-Tetrakis(pentafluorophenyl)porphyrinato]platinum(II) as an efficient, oxidation-resistant red phosphor: spectroscopic properties and applications in organic light-emitting diodes. *J Mater Chem*. 2003;13:1362–1366.
35. DeRosa MC, Mosher PJ, Yap GPA, Focsaneanu KS, Crutchley RJ, Evans CEB. Synthesis, characterization, and evaluation of [Ir(p-py)$_2$(vpy)Cl] as a polymer-bound oxygen sensor. *Inorg Chem*. 2003;42:4864–4872.
36. Wu WT, Wu WH, Ji SM, Guo HM, Wang X, Zhao JZ. The synthesis of 5,10,15,20-tetraarylporphyrins and their platinum(II) complexes as luminescent oxygen sensing materials. *Dyes Pigments*. 2011;89:199–211.
37. Biffinger JC, Kim HW, DiMagno SG. The polar hydrophobicity of fluorinated compounds. *Chembiochem*. 2004;5:622–627.

38. Chen X, Zhong ZM, Li Z, Jiang YQ, Wang XR, Wong K. Characterization of ormosil film for dissolved oxygen-sensing. *Sensor Actuators B*. 2002;87:233–238.
39. Song D, Kim H, Kim K. Measurement of dissolved oxygen concentration field in a microchannel using PtOEP/PS film. *J Visualization*. 2011;14:295–304.
40. Carraway ER, Demas JN, DeGraff BA, Bacon JR. Photophysics and photochemistry of oxygen sensors based on luminescent transition-metal complexes. *Anal Chem*. 1991;63:337–342.
41. Zhao Y, Ye TX, Chen HX, Huang DP, Zhou TY, He CY, Chen X. A dissolved oxygen sensor based on composite fluorinated xerogel doped with platinum porphyrin dye. *Luminescence*. 2011;26:29–34.
42. Guo ZQ, Nam S, Park S, Yoon J. A highly selective ratiometric near-infrared fluorescent cyanine sensor for cysteine with remarkable shift and its application in bioimaging. *Chem Sci*. 2012;3:2760–2765.
43. Wu W, Yao LM, Yang TS, Yin RY, Li FY, Yu YL. NIR-light-induced deformation of cross-linked liquid-crystal polymers using upconversion nanophosphors. *J Am Chem Soc*. 2011;133:15810–15813.
44. Shao JY, Sun HY, Guo HM, Ji SM, Zhao JZ, Wu WT, Yuan XL, Zhang CL, James TD. A highly selective red-emitting FRET fluorescent molecular probe derived from BODIPY for the detection of cysteine and homocysteine: an experimental and theoretical study. *Chem Sci*. 2012;3:1049–1061.
45. Avirah RR, Jayaram DT, Adarsh N, Ramaiah D. Squaraine dyes in PDT: from basic design to *in vivo* demonstration. *Org Biomol Chem*. 2012;10:911–920.

Manuscript received July 31, 2012, and revision received Feb. 7, 2013.